IN-CYLINDER MASS FLOW ESTIMATION AND MANIFOLD PRESSURE DYNAMICS FOR STATE PREDICTION IN SI ENGINES

Wojnar Sławomir, Boris Rohal'-Ilkiv*, Šimončič Peter, Honek Marek, Csambál Jozef

Slovak University of Technology in Bratislava, Faculty of Mechanical Engineering, Institute of Automation, Measurement and Applied informatics, Námestie slobody 17, 812 31 Bratislava, Slovakia

* corresponding author: boris.rohal-ilkiv@stuba.sk

Abstract. The aim of this paper is to present a simple model of the intake manifold dynamics of a spark ignition (SI) engine and its possible application for estimation and control purposes. We focus on pressure dynamics, which may be regarded as the foundation for estimating future states and for designing model predictive control strategies suitable for maintaining the desired air fuel ratio (AFR). The flow rate measured at the inlet of the intake manifold and the in-cylinder flow estimation are considered as parts of the proposed model. In-cylinder flow estimation is crucial for engine control, where an accurate amount of aspired air forms the basis for computing the manipulated variables. The solutions presented here are based on the mean value engine model (MVEM) approach, using the speed-density method. The proposed in-cylinder flow estimation method is compared to measured values in an experimental setting, while one-step-ahead prediction is illustrated using simulation results.

Keywords: combustion engine, AFR control, pressure dynamics, in-cylinder flow estimation, state prediction.
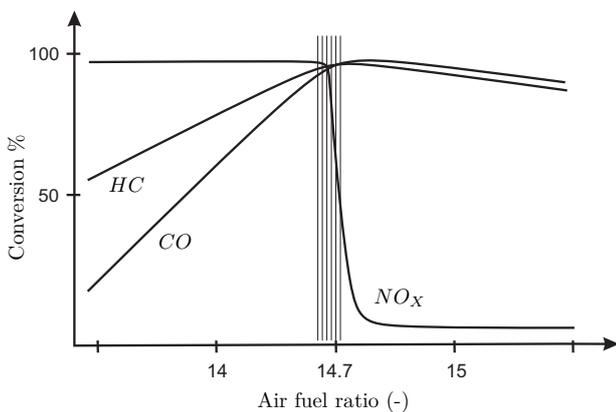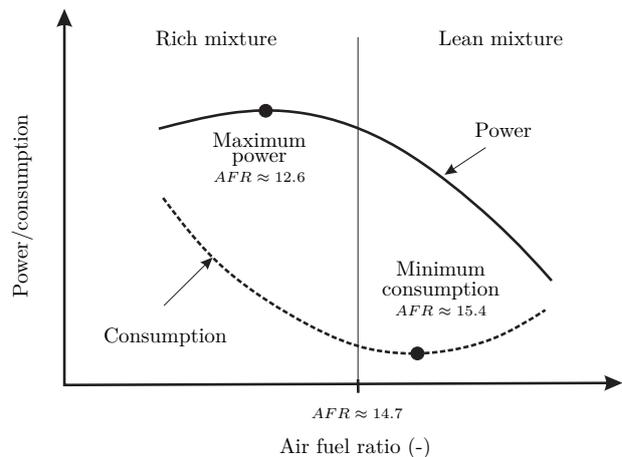
Figure 1. TWC conversion window.

Figure 2. Power and consumption depending on AFR.

1. Introduction

The use of three-way catalytic converters (TWC) in exhaust after-treatment systems of combustion engines is essential for reducing emissions to government established standards. However, to achieve maximum efficiency of TWC, the engine has to be cycled between lean and rich operating regimes (see Fig. 1) [1].

Not only the emission standards, but also the power and fuel consumption of a spark ignition (SI) engine need to be taken into account to satisfy consumer demands. To reach maximum power, the engine has to work with a rich mixture (air fuel ratio (AFR) ≈ 12.6), producing pollutants such as hydro carbons and carbon monoxide. However, if the engine works in regimes often described as minimal consumption (AFR ≈ 15.4), it will produce nitrogen oxides (see Fig. 2). The mutual dependance between power, con-

sumption and AFR has made AFR controllers more and more important, as they balance acceptable fuel economy with satisfactory power output, while minimizing the environmental impact [2, 3].

Because of the highly nonlinear dynamics of internal combustion engines, standard electronic control units (ECUs) cannot always produce the desired accurate control performance of the AFR. Ongoing research on AFR controllers includes solutions utilizing various advanced techniques, e.g. robust control [4], sliding mode control [5–7], or adaptive control [8–10]. In addition to these approaches, some proposed AFR controllers use advanced model-based approaches [1, 11–17]. Since the quality of model-based control depends strongly on accuracy, it is essential to create models that are as dependable as possible.
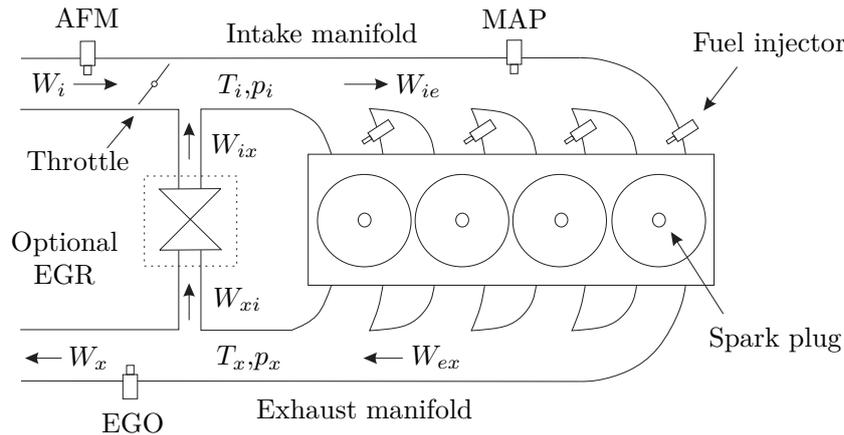
FIGURE 3. Simplified schematics of an SI engine.

This paper deals with modeling the air path, in response to the in-cylinder air mass flow estimation and intake flow measurements. Several works have analyzed estimations of the in-cylinder flow, enabling the air mass aspired into the combustion chamber to be estimated [18–20]. A state-of-the-art approach is to estimate the individual in-cylinder mass flow using periodic observers and Takagi-Sugeno design [21] or precise estimation of the injector characteristics [22]. However, certain modern algorithmic solutions are inherently complex, causing possible issues with real-time implementation, especially with predictive control. An alternative straightforward approach enables us to estimate the in-cylinder flow by applying the well known and widely used mean value engine model (MVEM) and the *speed-density* method. As this approach is computationally less expensive, it will be used throughout this paper.

The aim of this paper is to build a simple model that can be used as a basis for calculating predictions and thus for the design of an AFR predictive controller, asynchronous with the engine events. Many works deal with the air path dynamics of naturally aspired engines or turbo-charged engines, see e.g. [18, 23] and [24, 25]. Unlike works describing sampling synchronous with the engine events [26], we define a model describing pressure dynamics working asynchronously to engine events. As a result, the sampling of the proposed model is asynchronous. Due to its simplicity the in-cylinder mass flow estimation technique presented here utilizes direct differentiation, and a possible extension to usual observer design techniques can be found e.g. in [27]. As the test engine utilized in the experiment does not feature variable valve timing (VVT) or exhaust gas recirculation (EGR), the proposed solutions are shown without considering these effects. Moreover, because a practical analysis would be troublesome, this work does not consider the effect of thermal transients.

This paper is organized in the following fashion. In Section 2, the dynamics of the air path is considered and its connection with the intake manifold and the in-cylinder flows are presented. Section 3 describes the structure of the model predictions and the experimental computation of the in-cylinder flow estimation compared to measurement. Certain preliminary experimental and simulation results are presented in Section 4.

2. MODEL OF THE AIR SYSTEM

The model for the air fuel ratio consists of two independent parts: the air and the fuel system of the SI engine. However, only the air system is taken into consideration in this paper. The model is conceptually illustrated in Fig. 3. The variables have the following meaning: W variables deal with the mass flows, W_i into the intake manifold (through the throttle), W_{ie} from the intake manifold to the engine, W_{ex} from the engine to the exhaust manifold, W_x out of the exhaust manifold, W_{ix} from the EGR to the intake manifold, and W_{xi} from the exhaust manifold to the EGR. T_i, p_i describe the temperature and pressure in the intake manifold, and T_x, p_x denote the temperature and the pressure in the exhaust manifold.

2.1. INTAKE MANIFOLD PRESSURE DYNAMICS

The dynamics of the pressure in the intake manifold can be described by an equation based on the ideal gas law, internal energy and enthalpy equations [18, 23]. Applying the ideal gas law gives us:

$$p(t)V = n(t)\tilde{R}T(t), \tag{1}$$

where p is pressure, V is volume, n is the amount of substance in the moles, $\tilde{R}$ is the ideal gas constant (denoted with a tilde '~' to keep the notation uniform), and T is the gas temperature (in Kelvins).

Since it is physically easier to measure mass, the number of moles n is not a suitable variable for further computation, and we will express it as mass m divided by the molar mass M:
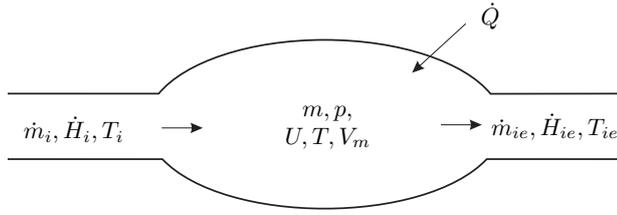
$$n(t) = \frac{m(t)}{M}. \tag{2}$$

FIGURE 4. Input, states and outputs in an intake manifold model.

In this way we can transform (1) into:

$$p(t)V = m(t)\frac{\tilde{R}}{M}T(t) = m(t)RT(t). \qquad (3)$$

The internal energy of a system is equal to

$$U(t) = c_{\mathrm{v}}T(t)m(t), \qquad (4)$$

where c_{v} is the specific heat at a constant volume.

If one analyzes the intake manifold system presented in Fig. 4 and substitutes $T(t)m(t)$ in (4) with (3) and assumes that V is equal to manifold volume V_{m}, then we obtain:

$$U(t) = c_{\mathrm{v}}\frac{p(t)V_{\mathrm{m}}}{R}. \qquad (5)$$

The fundamental equation describing the physics of gases assumes that $R = c_p - c_v$ and $\kappa = \frac{c_p}{c_v}$. Then $\frac{c_v}{R}$ in (5) is equal to $\frac{c_v}{c_p - c_v} = \frac{1}{\frac{c_p}{c_v} - 1} = \frac{1}{\kappa - 1}$, and (5) derives into:

$$U(t) = \frac{1}{\kappa - 1}p(t)V_{\mathrm{m}}. \qquad (6)$$

In the next step, the enthalpy of the system is described as

$$\dot{H}_{\mathrm{i}}(t) = c_{\mathrm{p}}\dot{m}_{\mathrm{i}}(t)T_{\mathrm{i}}(t) = c_{\mathrm{p}}W_{\mathrm{i}}(t)T_{\mathrm{i}}(t), \qquad (7)$$

$$\dot{H}_{\mathrm{ie}}(t) = c_{\mathrm{p}}\dot{m}_{\mathrm{ie}}(t)T_{\mathrm{ie}}(t) = c_{\mathrm{p}}W_{\mathrm{ie}}(t)T_{\mathrm{ie}}(t), \qquad (8)$$

where c_{p} is the specific heat at a constant pressure. Applying the change of the internal energy gives:

$$\frac{d}{dt}U(t) = \dot{H}_{\mathrm{i}}(t) - \dot{H}_{\mathrm{in}}(t) + \dot{Q}(t). \qquad (9)$$

If one substitutes equations (7) and (8) into (9), and assumes that there is no heat transfer through the walls of the intake manifold ($\dot{Q}(t) = 0$ in Fig. 4):

$$\frac{1}{\kappa - 1}\dot{p}(t)V_{\mathrm{m}} = c_{\mathrm{p}}W_{\mathrm{i}}(t)T_{\mathrm{i}}(t) - c_{\mathrm{p}}W_{\mathrm{ie}}(t)T_{\mathrm{ie}}, \qquad (10)$$

and after transformation:

$$\dot{p}(t) = \frac{c_{\mathrm{p}}(\kappa - 1)}{V_{\mathrm{m}}}\big(W_{\mathrm{i}}(t)T_{\mathrm{i}}(t) - W_{\mathrm{ie}}(t)T_{\mathrm{ie}}\big), \qquad (11)$$

where $c_p(\kappa - 1) = c_p\kappa - c_p = c_p\kappa - c_v\kappa = (c_p - c_v)\kappa = R\kappa$. After substituting $c_p(\kappa - 1)$ into (11) we obtain the dynamic equation describing the pressure in the intake manifold:

$$\dot{p}(t) = \frac{R_{\mathrm{air}}\kappa}{V_{\mathrm{m}}}\big(W_{\mathrm{i}}(t)T_{\mathrm{i}}(t) - W_{\mathrm{ie}}(t)T_{\mathrm{ie}}\big). \qquad (12)$$

In further sections both the flow measured at the inlet of the intake manifold W_{i} and the in-cylinder flow W_{ie} will be considered.
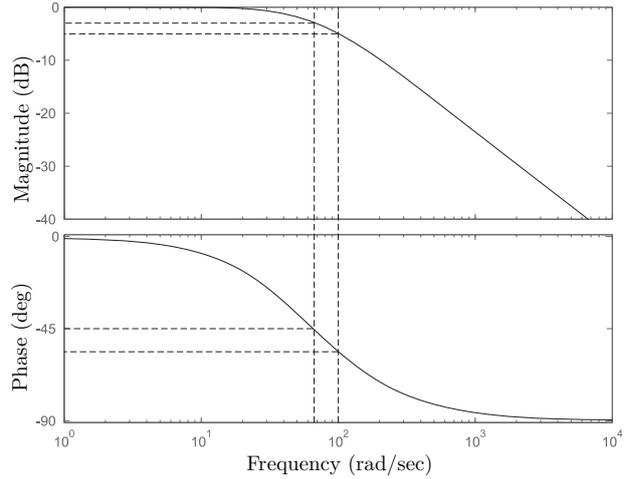

FIGURE 5. Bode diagram for the transfer function $G(s)$.

2.2. AIR MASS FLOW MEASUREMENT

In this section, we take into account the input to the differential equation given by Eq. (12), described as the flow measured at the inlet of the intake manifold W_{i}, or the flow through the throttle. The dynamics of the air flow mass meter were modeled by the following equation [18, 20]:

$$MAF_{\mathrm{i}}(t) = MAF_{\mathrm{md}}(t) + \tau\frac{d}{dt}MAF_{\mathrm{md}}(t), \qquad (13)$$

where MAF_{i} is the actual air mass flow, MAF_{md} is the measured air mass flow, and τ is a time lag equal to about 15 ms. A disadvantage of this approach is that the presented estimation may amplify the high frequency noise present in the sensor measurements [7].

Since Eq. (13) describes first order system dynamics with a time constant (equal to τ), the system can be described by the transfer function

$$G(s) = \frac{1}{0.015s + 1}. \qquad (14)$$

If one analyzes the Bode diagrams (see Fig. 5) of the system in (14), one may notice that at frequencies higher than 8 Hz (50 rad/s) the signal amplitude starts to be attenuated.

A frequency equal to 8 Hz appears in the intake manifold when the rotation speed of the engine is twice as fast as the frequency registered in the manifold. This is caused by the fact that during one turn of a crankshaft (360 deg) two intake strokes take place. This means that a frequency of 8 Hz appears at an engine speed equal to 1000 revolutions per minute (rpm). The corresponding phase attenuation is equal to 45 deg (see Fig. 5). Since a typical gasoline engine usually works with speeds higher than 1000 rpm, the phase is also decreased and (as can be seen in Fig. 5) it can reach about −55 deg.

Note that the air mass flow into the manifold W_{i} (see Fig. 3) is in this case measured with the AFM. However, it can be expressed as a function of the throttle position, and the difference between the pressure

in front of the throttle and behind it:

$$W_{\mathrm{i}} = A_{\mathrm{th}} \frac{p_{\mathrm{a}}}{R_{\mathrm{air}} T_{\mathrm{a}}} \sqrt{\frac{2\kappa}{\kappa-1}\left[\left(\frac{p_{\mathrm{im}}}{p_{\mathrm{a}}}\right)^{\frac{2}{\kappa}} - \left(\frac{p_{\mathrm{im}}}{p_{\mathrm{a}}}\right)^{\frac{\kappa-1}{\kappa}}\right]}, \quad (15)$$

where the 'im' indexes refer to the intake manifold conditions and the 'a' indexes refer to the ambient conditions. A_{th} is a flow section through the throttle and is a function of the throttle angle $A_{\mathrm{th}} = f(\alpha)$, while κ is Poisson's constant.

2.3. Cylinder Flow Computation

In-cylinder flow estimation is based on the idea of using the reading from the manifold absolute pressure sensor (MAP) in the flow computation [18, 19, 24, 28]. An MAP sensor is mounted closer to the cylinders (valves) than the AFM sensor, and it prevents the influence of air accumulation in the manifold. As a result, the in-cylinder flow can be estimated more accurately, especially in transient regimes. The basis for flow estimation [3] is Eq. (16):

$$\dot{m}_{\mathrm{mix}}(t) = \rho_{\mathrm{in}}(t) \cdot \dot{V}_{\mathrm{d}}(t)$$
$$= \rho_{\mathrm{in}}(t) \cdot \eta_{\mathrm{v}}(p, rev)\frac{V_{\mathrm{d}}}{60N}n_{\mathrm{e}}(t), \quad (16)$$

where $\dot{m}$ will from now on be denoted by W, ρ_{in} is the density of the gas at the intake of the engine, η_{v} is volumetric efficiency, V_{d} is displaced volume, n_{e} is engine speed and N is the number of revolutions per one cycle ($N = 2$ for four stroke engines). Volumetric efficiency depends on engine speed and load (expressed as pressure).

If we use density $\rho_{\mathrm{in}}(t)$ in the form

$$\rho_{\mathrm{in}}(t) = \frac{p_{\mathrm{in}}(t)}{R_{\mathrm{in}} T_{\mathrm{in}}(t)} \quad (17)$$

and substitute it into (16), we obtain:

$$W_{\mathrm{mix}}(t) = \eta_{\mathrm{v}}(p, rev)\frac{p_{\mathrm{in}}(t)}{R_{\mathrm{in}} T_{\mathrm{in}}(t)}\frac{V_{\mathrm{d}}}{60N}n_{\mathrm{e}}(t), \quad (18)$$

where p is absolute air pressure, R is the ideal gas constant, T is gas temperature (in Kelvins) and the 'in' indexes refer to the conditions at the intake of the engine.

Note that the gas density ρ_{in} in (17) refers to the conditions at the inlet of the intake manifold. In a real experiment we can measure the pressure and the temperature in the manifold. These refer to the manifold density ρ_{m}, which can be expressed as

$$\rho_{\mathrm{m}}(t) = \frac{p_{\mathrm{m}}(t)}{R_{\mathrm{m}} T_{\mathrm{m}}(t)}, \quad (19)$$

where the 'm' indexes refer to conditions in the manifold.

If one rewrites Eq. (18) and substitutes ρ_{in} with ρ_{m} and aims to have W_{mix} unchanged, then one has to change the meaning of volumetric efficiency η_{v}. Thus, now the new volumetric efficiency is related to the

manifold conditions, and is marked as $\tilde{\eta}_{\mathrm{v}}$. As is shown in Fig. 9, the aspired mixture consists of air and fuel, so it is necessary to compute the gas constant R and the temperature T related to the mixture:

$$R_{\mathrm{mix}} = \frac{(\dot{m}_{\mathrm{air}} \cdot R_{\mathrm{air}}) + (\dot{m}_{\mathrm{fuel}} \cdot R_{\mathrm{fuel}})}{\dot{m}_{\mathrm{air}} + \dot{m}_{\mathrm{fuel}}} \quad (20)$$

$$T_{\mathrm{mix}} = \frac{(\dot{m}_{\mathrm{air}} \cdot T_{\mathrm{air}} \cdot c_{\mathrm{pair}}) + (\dot{m}_{\mathrm{fuel}} \cdot T_{\mathrm{fuel}} \cdot c_{\mathrm{p,fuel}})}{(\dot{m}_{\mathrm{air}} \cdot c_{\mathrm{pair}}) + (\dot{m}_{\mathrm{fuel}} \cdot c_{\mathrm{p,fuel}})} \quad (21)$$

where: c_{air} and $c_{\mathrm{p,fuel}}$ are the specific heat of air and fuel at constant pressure.

If we substitute Equations (20), (21) into (18), subtract the fuel flow (W_{f}) from the air flow (18) and take the changed volumetric efficiency into consideration, we obtain the equation describing the in-cylinder flow:

$$W_{\mathrm{ie}}(t) = \tilde{\eta}_{\mathrm{v}}(p, rev)\frac{p_{\mathrm{m}}(t)}{R_{\mathrm{mix}} T_{\mathrm{mix}}(t)}\frac{V_{\mathrm{d}}}{60N}n_{\mathrm{e}}(t) - W_{\mathrm{f}}(t). \quad (22)$$

The fuel flow that appears in Eq.(22) is defined as:

$$W_{\mathrm{f}} = IIR \cdot IF, \quad (23)$$

where IF is the characteristic injector flow and IIR is the ratio of the injection length to the intake stroke length:

$$IIR = \frac{(\text{pulse width})}{(\text{intake length})}. \quad (24)$$

2.4. Volumetric Efficiency Estimation

Volumetric efficiency $\tilde{\eta}_{\mathrm{v}}$ is a crucial variable, which influences the flow into the cylinders. It describes how much air can be aspired into the chamber in comparison with the volume of the combustion chamber. It is a nonlinear parameter and is a function of the engine speed and load ($\tilde{\eta}_{\mathrm{v}}(rev, load)$) [3]. The goal of this section is to describe the estimation routine of this factor.

Since the air in the intake manifold has a dynamic character, the air mass flow to intake manifold W_{i} does not have to be equal to the cylinder air flow W_{ie} in the transient regime (see Fig. 3). However, in steady states, these two flows are equal because there is no other source charging the manifold with air, and there is no other outflow. Thus, it is possible to substitute in Eq. (22) the measurement from the AFM (W_{i}) by the estimated in-cylinder flow (W_{ie}):

$$W_{\mathrm{i}}(t) = \tilde{\eta}_{\mathrm{v}}(p, rev)\frac{p_{\mathrm{m}}(t)}{R_{\mathrm{mix}} T_{\mathrm{mix}}(t)}\frac{V_{\mathrm{d}}}{60N}n_{\mathrm{e}}(t) - W_{\mathrm{f}}(t) \quad (25)$$

We have obtained an equation with one unknown variable — $\tilde{\eta}_{\mathrm{v}}$. This can be inserted on the left side of the equation and thus the volumetric efficiency can be computed as a dependance of AFM-measurement, MAP sensor reading, manifold temperature and engine speed:

$$\tilde{\eta}_{\mathrm{v}}(p, rev) = \frac{60\big(W_{\mathrm{i}}(t) - W_{\mathrm{f}}(t)\big)R_{\mathrm{mix}} T_{\mathrm{mix}}(t)N}{p_{\mathrm{m}}(t)V_{\mathrm{d}}n_{\mathrm{e}}(t)} \quad (26)$$
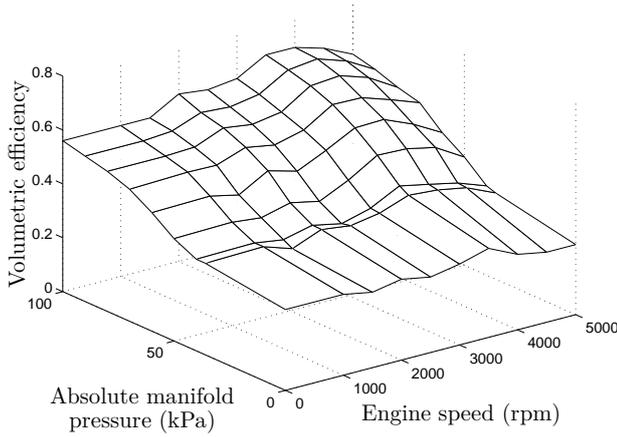
FIGURE 6. Measured volumetric efficiency map.

A two dimensional map of the volumetric efficiency estimated this way can be used in transient regimes to compute the in-cylinder flow. In dependence on changing revolutions and loads, the volumetric efficiency also changes and influences the estimated flow (see Fig. 6). The presented map shows the volumetric efficiency $\tilde{\eta}_{\mathrm{v}}$ estimated in every 500 revolutions and every 10 kPa. Of course, the volumetric efficiency maps of different engines differ. If one needs a more accurate map, one may estimate it with higher resolution (for example every 5 kPa, or every 250 revolutions), or use higher resolution in areas with a strongly nonlinear character, and lower resolution in less nonlinear areas. The volumetric efficiency map presented in Fig. 6 is based on a measurement which was carried out on a test bench with an SI combustion engine made by Volkswagen (1.4 liter volume, 16 valves, 55 kW power).

2.5. SUMMARY OF MODELS

In Sections 2.2 and 2.3, both components of the dynamic model were considered. If we substitute Eqs. (22) and (13) into (12), the pressure dynamics can be expressed as

$$\dot{p}(t) = \frac{R_{\mathrm{air}} T_{\mathrm{i}}(t)\kappa}{V_{\mathrm{m}}} \Big(W_{\mathrm{i}}(t) + \tau \frac{d}{dt} W_{\mathrm{i}}(t) \Big) - \tilde{\eta}_{\mathrm{v}}(p, rev) p(t) \frac{R_{\mathrm{air}} T_{\mathrm{ie}}(t)}{R_{\mathrm{mix}} T_{\mathrm{mix}}(t)} \frac{V_{\mathrm{d}}}{V_{\mathrm{m}}} \frac{n_{\mathrm{e}}(t)}{2}. \quad (27)$$

Since we want to apply the equation in a discrete time control system, we are interested in its discrete time implementation. To solve this problem, we have used the typical Euler numerical procedure for solving ordinary differential equations. The solution looks as follows:

$$p(k) = p(k-1) + \delta T \Big(\frac{R_{\mathrm{air}} T_{\mathrm{i}}(k)\kappa}{V_{\mathrm{m}}} \Big(W_{\mathrm{i}}(k-1) + \tau \frac{W_{\mathrm{i}}(k-1) - W_{\mathrm{i}}(k-2)}{\delta T} \Big) - \tilde{\eta}_{\mathrm{v}}(p, rev) p(k-1) \frac{R_{\mathrm{air}} T_{\mathrm{ie}}\kappa}{R_{\mathrm{mix}} T_{\mathrm{mix}}} \frac{V_{\mathrm{d}}}{V_{\mathrm{m}}} \frac{n_{\mathrm{e}}(k)}{2} - W_{\mathrm{f}}(k) \Big), \quad (28)$$

where δT is the sampling period, k is the sample number, p is the system state and W_{i} is the input.

The analysis of (28) shows that the pressure in the intake manifold can be simulated depending on the past pressure values, input — flow through the AFM, and further variables, such as temperature and engine speed.

3. PREDICTION WITH THE MODEL

The dynamics of the air system presented in the previous sections offers the possibility to predict future states of the system. It is obvious that equation (28) can be rewritten in the form of a one-step-ahead prediction, that is:

$$\hat{p}(k+1) = p(k) + \delta T \Big(\frac{R_{\mathrm{air}} T_{\mathrm{i}}(k)}{V_{\mathrm{m}}} \Big(W_{\mathrm{i}}(k) + \tau \frac{W_{\mathrm{i}}(k) - W_{\mathrm{i}}(k-1)}{\delta T} \Big) - \tilde{\eta}_{\mathrm{v}}(p, rev) p(k) \frac{R_{\mathrm{air}} T_{\mathrm{ie}}(k)}{R_{\mathrm{mix}} T_{\mathrm{mix}}(k)} \frac{V_{\mathrm{d}}}{V_{\mathrm{m}}} \frac{n_{\mathrm{e}}(k)}{2} - W_{\mathrm{f}}(k) \Big), \quad (29)$$

where pressure $p(k)$ and other variables measured at a discrete sample time k enable future states $\hat{p}(k+1)$ to be predicted.

If one wants to increase the prediction accuracy, it is possible to define a model of the temperature and the engine speed and insert them into Eq. (29). Since we have focused on the air path dynamics, we have used a simplification assuming that the engine speed and the temperatures are constant. The many-step-ahead prediction is then defined as

$$\hat{p}(k+i+1) = \hat{p}(k+i) + \delta T \Big(\frac{R_{\mathrm{air}} T_{\mathrm{i}}(k)}{V_{\mathrm{m}}} \Big(W_{\mathrm{i}}(k) + \tau \frac{W_{\mathrm{i}}(k) - W_{\mathrm{i}}(k-1)}{\delta T} \Big) - \tilde{\eta}_{\mathrm{v}}(p, rev) \hat{p}(k+i) \frac{R_{\mathrm{air}} T_{\mathrm{ie}}(k)}{R_{\mathrm{mix}} T_{\mathrm{mix}}(k)} \frac{V_{\mathrm{d}}}{V_{\mathrm{m}}} \frac{n_{\mathrm{e}}(k)}{2} - W_{\mathrm{f}}(k) \Big). \quad (30)$$

The predicted pressure can then be used in air flow computations. If we substitute $\hat{p}(k+1)$ in Eq. (22) we obtain:

$$\hat{W}_{\mathrm{ie}}(k+i) = \tilde{\eta}_{\mathrm{v}}(p, rev) \frac{\hat{p}_{\mathrm{m}}(k+i)}{R_{\mathrm{mix}} T_{\mathrm{mix}}(k)} \frac{V_{\mathrm{d}}}{60N} n_{\mathrm{e}}(k) - W_{\mathrm{f}}(k). \quad (31)$$

Supposing that the engine speed is constant, the intake stroke length can be easily computed. If we integrate flows $\hat{W}_{\mathrm{ie}}(k+i)$ on a horizon $(k$ to $k+i)$, $(k+i$ to $k+2i)$, $(k+ni$ to $k+(n+1)i)$ and so on (see Fig. 7), it will be possible to compute the mass of air aspired to the combustion chamber in future intake strokes $\hat{m}(n)$ (where i is the determined amount of prediction, and n is the number of predicted intake strokes).
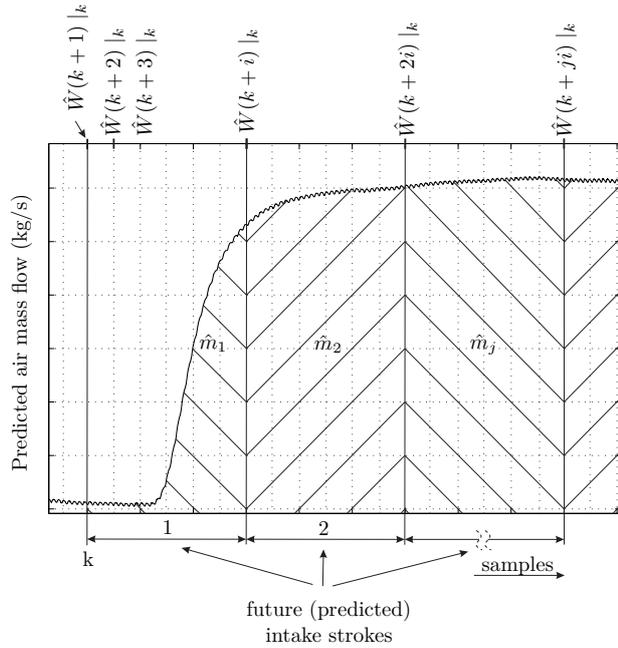
FIGURE 7. Air mass flow prediction on a desired amount of assumed intake strokes.

The following equation describes the vector of predicted masses:

$$\hat{\boldsymbol{m}}(n) = \sum_{i=0}^{set} \hat{W}_{\text{ie}}(n \cdot set + i)t_{\text{pred}}, \qquad (32)$$

where $t_{\text{pred}} = it/set$ is the time equal to an intake stroke time divided by the number of prediction steps, it is the intake stroke time, set is a parameter which changes the accuracy of the computations (defining the number of samples in one predicted intake stroke). According to this definition, the model can be computed asynchronously to the engine events — with sampling periods independent from engine speed. However, in every computation period a constant number of future intakes (or aspired masses) are predicted. Note that n varies from 0 to the max amount of intake strokes that are predicted, and i varies from 0 to max number of integration steps.

Note that the volumetric efficiency changes with the following iteration steps. These changes are not accurate, because the volumetric efficiency depends on the engine speed and pressure, and we predict only the pressure changes. Importantly, volumetric efficiency is the main source of nonlinearity that influences both the pressure dynamics and the air mass flow into the chamber.

4. EXPERIMENTAL AND NUMERICAL RESULTS

The in-cylinder flow estimation was evaluated experimentally on the test bench with a Volkswagen SI engine. Fig. 8 compares the air flow measured in the inlet pipe with AFM (W_{i}) with the air flow obtained by the speed-density calculation (W_{ie}).
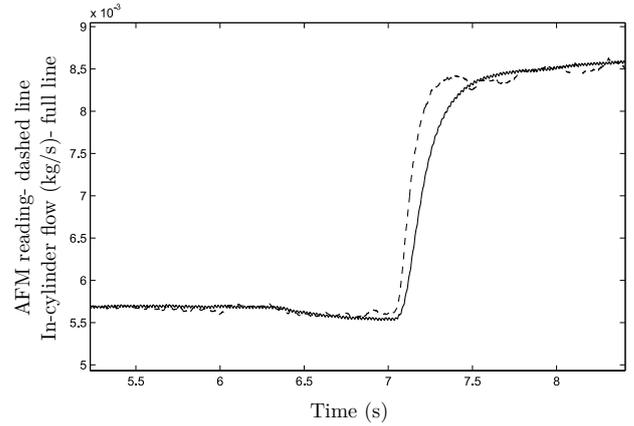

FIGURE 8. Measurement with AFM is denoted by a dashed line, computed air mass flow with a full line.
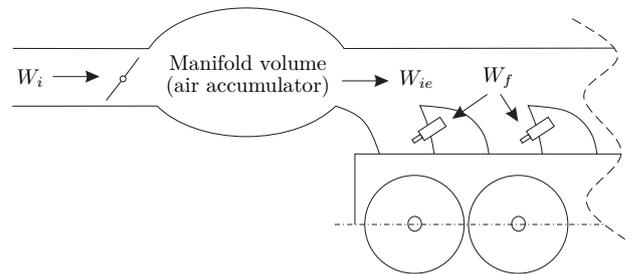

FIGURE 9. Schematic representation of the intake manifold.

Note that since the actual flow into the engine cannot be measured in a straightforward way, the quality of the estimation cannot be independently judged. In a steady state, when no other source is charging the manifold with air, and no other outflow appears, the accuracy of the estimation is obvious. The intake manifold has a relatively big volume, which acts as an air accumulator (see Fig. 9). After the throttle opens, it has to be filled with air and then air can be aspired into the cylinder. A difference therefore appears between W_{i} and W_{ie} in the transient regime. In this regime, the air accumulation also has to be taken into consideration.

Since the aim of this paper is to define a model which can be utilized as a basis for predicting system states, a one-step-ahead prediction of the pressure is presented here. Figure 10 shows the simulated pressure with a full line, and the predicted pressure with a dotted line.

Prediction of the aspired air masses in future strokes will not be presented here. Since the prediction algorithm runs asynchronously with engine events, it is difficult to compare its results with the mass of air aspired to the chamber. Moreover, it would be interesting to analyze the future aspired masses in a transient regime. The underlying problem here is that the revolutions are not exactly constant in a real test-run and a prediction gap appears, which is caused by the assumption that the revolutions are constant throughout the horizon (see Sect. 3). However, in the
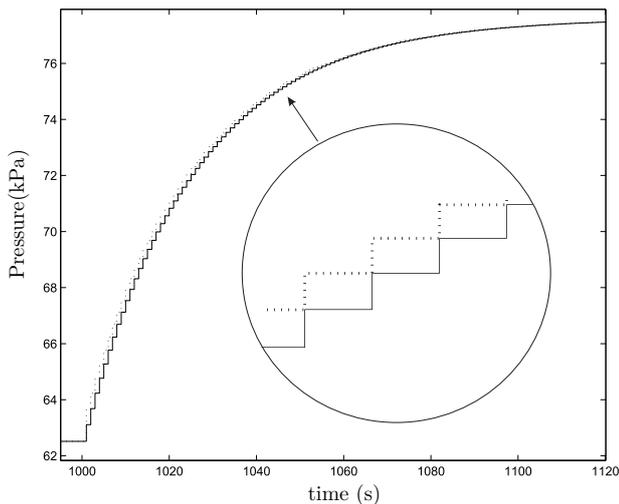
FIGURE 10. One step ahead prediction of the pressure.

simulations the predictions are completely accurate — similar to the prediction presented in Fig. 10.

5. CONCLUSION

A model of the intake manifold dynamics has been presented in this work. We have described its usage in control and simulation. A comparison of the intake and in-cylinder flows measured on a test bench with a real SI engine have also been presented.

An important topic for future research will be to apply the model presented here in a model-based AFR predictive control scheme. Further efforts will be focused on using the preliminary results achieved in the works of [12] and [13] in designing an AFR predictive controller. This paper deals only with an engine model without an exhaust gas recirculation (EGR) valve or turbocharger. Turbo-charged engines have become especially interesting, and might be an attractive research topic. The presented air system (see Fig. 3) would have to be extended with equations describing the exhaust manifold conditions ($W_{\mathrm{exm}}(t)$ and $\dot{p}_{\mathrm{exm}}(t)$). Then the flow through the EGR and the turbocharger will influence the intake manifold conditions ($W_{\mathrm{inm}}(t)$ and $\dot{p}_{\mathrm{inm}}(t)$), and there will be a need to reformulate the model presented here. Some of these issues are currently being investigated by the authors.

REFERENCES

[1] K. R. Muske, J. C. P. Jones. Feedforward/feedback air fuel ratio control for an automotive catalyst. In *Proceedings of the 2003 American Control Conference*, pp. 1386–1391. Denver, Colorado, USA, 2003. DOI:10.1109/ACC.2003.1239784.

[2] P. Andersson. *Intake Air Dynamics on a Turbocharged SI-Engine with Wastegate.* Master's thesis, Linkoping University, Sweden, 2002.

[3] L. Guzzella, C. Onder. *Introduction to Modeling and Control of IC Engine Systems.* Springer, 2010. DOI:10.1007/978-3-642-10775-7.

[4] C. W. Vigild, K. P. H. Andersen, E. Hendricks. Towards robust h-infinity control of an si-engine's air/fuel ratio. *SAE Technical Paper No 1999-01-0854* 1999. DOI:10.4271/1999-01-0854.

[5] J. K. Pieper, R. Mehrotra. Air/fuel ratio control using sliding mode methods. In *American Control Conference*, pp. 1027–1031. San Diego, CA, USA, 1999. DOI:10.1109/ACC.1999.783196.

[6] J. K. H. J. S. Souder. Adaptive sliding mode control of air-fuel ratio in internal combustion engines. *International Journal of Robust and Nonlinear Control* **14**(6):525–541, 2004. DOI:10.1002/rnc.901.

[7] S. W. Wang, D. L. Yu. A new development of internal combustion engine air-fuel ratio control with second-order sliding mode. *Journal of Dynamic systems, Measurement and Control* **129**(6):757–766, 2007. DOI:10.1115/1.2789466.

[8] S. W. Wang, D. L. Yu. Adaptive air-fuel ratio control with MLP network. *International Journal of Automation and Computing* **2**(2):125–133, 2005. DOI:10.1007/s11633-005-0125-y.

[9] K. R. Muske, J. C. P. Jones, E. M. Franceschi. Adaptive analytical model-based control for si engine air-fuel ratio. *IEEE Transactions on Control Systems Technology* **16**(4):763–768, 2008. DOI:10.1109/TCST.2007.912243.

[10] Y. Yildiz, A. Annaswamy, D. Yanakiev, I. Kolmanovsky. Spark ignition engine fuel-to-air ratio control: An adaptive control approach. *Control Engineering Practice* **18**:1369–1378, 2010. DOI:10.1016/j.conengprac.2010.06.011.

[11] K. R. Muske, J. C. P. Jones. A model-based si engine air-fuel ratio contoller. In *Proceedings of the 2006 American Control Conference*, pp. 3284–3289. Minneapolis, Minnesota, USA, 2006. DOI:10.1109/ACC.2006.1657224.

[12] T. Polóni, other. Multiple arx model-based air-fuel ratio predictive control for si engines. In *3rd IFAC Workshop on Advanced Fuzzy and Neural Control.* Valenciennes, France, 2007. DOI:10.3182/20071029-2-FR-4913.00013.

[13] T. Polóni, other. Modeling of air-fuel ratio dynamics of gasoline combustion engine with arx network. *Journal of Dynamic Systems, Measurement and Control-Transactions of the ASME* **130**(6):061009/1–061009/10, 2008. DOI:10.1115/1.2963049.

[14] E. Alfieri, A. Amstutz, L. Guzzella. Gain-scheduled model-based feedback control of the air/fuel ratio in diesel engines. *Control Engineering Practice* **17**:1417–1425, 2009. DOI:10.1016/j.conengprac.2008.12.008.

[15] L. del Re, F. Allgöwer, L. Glielmo, et al. (eds.). *Automotive Model Predictive Control: Models, Methods and Applications*, vol. 402 of *Lecture Notes in Control and Information Sciences*. Springer-Verlag Berlin Heidelberg, 2010. DOI:10.1007/978-1-84996-071-7.

[16] S. Behrendt, P. Dunow, P. Lampe. An application of model predictive control to a gasoline engine. In M. Fikar, M. Kvasnica (eds.), *Proceedings of the 18th International Conference on Process Control*, pp. 57 – 63. Hotel Titris, Tatranská Lomnica, Slovakia, 2011.

[17] H. C. Wong, P. K. Wong, C. M. Vong. Model predictive engine air-ratio control using online sequential relevance vector machine. *Journal of Control Science and Engineering* p. 15, 2012. Hindawi Publishing Corporation, DOI:10.1155/2012/731825.

[18] A. A. Stotsky, I. Kolmanovsky. Application of input estimation techniques to charge estimation and control in automotive engines. *Control Engineering Practice* **10**:1371–1383, 2002. DOI:10.1016/S0967-0661(02)00101-6.

[19] J. Desantes, J. Galindo, C. Guardiola, V. Dolz. Air mass flow estimation in turbocharged diesel engines from in-cylinder pressure measurement. *Experimental Thermal and Fluid Science* **34**(1):37–47, 2012. DOI:10.1016/j.expthermflusci.2009.08.009.

[20] J. Grizzle, J. Cook, W. Milam. Improved cylinder air charge estimation for transient air fuel ratio control. In *Preceedings of the American Control Conference*, vol. 2, pp. 1568–1573. Baltimore USA, 1994. DOI:10.1109/ACC.1994.752333.

[21] H. Kerkeni, J. Lauber, T. Guerra. Estimation of individual in-cylinder air mass flow via periodic observer in takagi-sugeno form. In *Vehicle Power and Propulsion Conference (VPPC) 2012, IEEE*, pp. 1–6. Lille, France, 2010. DOI:10.1109/VPPC.2010.5729154.

[22] L. Benvenuti, M. Di Benedetto, S. Di Gennaro, A. Sangiovanni-Vincentelli. Individual cylinder characteristic estimation for a spark injection engine. *Automatica* **39**(7):1157–1169, 2003. DOI:10.1016/S0005-1098(03)00077-3.

[23] A. A. Stotsky. *Automotive engines: Control, Estimation, Statistical detection.* Automotive engines. Springer-Verlag, Berlin Heidelberg, 2009. DOI:10.1007/978-3-642-00164-2.

[24] M. Jung. *Mean-Value Modelling and Robust Control of the Airpath of a Turbocharged Diesel Engine.* Ph.D. thesis, Sidney Sussex College, Department of Engineering, University of Cambridge, Trumpington Street, Cambridge, UK, 2003.

[25] P. Andersson, L. Eriksson. Air-to-cylinder observer on a turbocharged si-engine with wastegate. In *Proceedings of SAE 2001 World Congress.*, 2001-01-0262, pp. 33–40. Detroit, MI, USA, 2001. DOI:10.4271/2001-01-0262.

[26] T. Jimbo, Y. Hayakawa. A physical model for engine control design via role state variables. *Control Engineering Practice* **19**(3):276–286, 2011. DOI:10.1016/j.conengprac.2010.03.008.

[27] O. Barbarisi, A. di Gaeta, L. Glielmo, S. Santini. An extended kalman observer for the in-cylinder air mass flow estimation. In *Proceedings of the MECA02 International Workshop on Diagnostics in Automotive Engines and Vehicles*, pp. 1–14. University of Salerno, Fisciano (SA), Italy, 2002.

[28] S. Di Cairano, D. Yanakiev, A. Bemporad, et al. *Model Predictive Powertrain Control: An Application to Idle Speed Regulation*, pp. 183–194. Springer, 2010. DOI:10.1007/978-1-84996-071-7_12.